Stem Cell Reports
Resource
OPEN ACCESS

A 3D Sphere Culture System Containing Functional Polymers for Large-Scale Human Pluripotent Stem Cell Production

Tomomi G. Otsuji,[1,6] Jiang Bin,[1,6] Azumi Yoshimura,[1] Misayo Tomura,[2] Daiki Tateyama,[3] Itsunari Minami,[1] Yoshihiro Yoshikawa,[3] Kazuhiro Aiba,[1] John E. Heuser,[1] Taito Nishino,[2] Kouichi Hasegawa,[1,4] and Norio Nakatsuji[1,5,*]

[1]Institute for Integrated Cell-Material Sciences (WPI-iCeMS), Kyoto University, Ushinomiya-cho, Yoshida, Sakyo-ku, Kyoto 606-8501, Japan
[2]Nissan Chemical Industries, Ltd., 3-7-1 Kanda Nishiki-cho, Chiyoda-ku, Tokyo 101-1154, Japan
[3]Nipro Corporation, 3023 Noji-cho, Kusatsu, Shiga 525-0055, Japan
[4]Institute for Stem Cell Biology and Regenerative Medicine, National Centre for Biological Sciences, GKVK, Bellary Road, Bangalore 560065, India
[5]Institute for Frontier Medical Sciences, Kyoto University, 53 Kawahara-cho, Sakyo-ku, Kyoto 606-8507, Japan
[6]These authors contributed equally to this work
*Correspondence: nnakatsu@icems.kyoto-u.ac.jp
http://dx.doi.org/10.1016/j.stemcr.2014.03.012

SUMMARY

Utilizing human pluripotent stem cells (hPSCs) in cell-based therapy and drug discovery requires large-scale cell production. However, scaling up conventional adherent cultures presents challenges of maintaining a uniform high quality at low cost. In this regard, suspension cultures are a viable alternative, because they are scalable and do not require adhesion surfaces. 3D culture systems such as bioreactors can be exploited for large-scale production. However, the limitations of current suspension culture methods include spontaneous fusion between cell aggregates and suboptimal passaging methods by dissociation and reaggregation. 3D culture systems that dynamically stir carrier beads or cell aggregates should be refined to reduce shearing forces that damage hPSCs. Here, we report a simple 3D sphere culture system that incorporates mechanical passaging and functional polymers. This setup resolves major problems associated with suspension culture methods and dynamic stirring systems and may be optimal for applications involving large-scale hPSC production.

INTRODUCTION

Human pluripotent stem cells (hPSCs), including human embryonic stem cells (hESCs) and human induced pluripotent stem cells (hiPSCs), hold great promise in the fields of regenerative medicine and drug discovery. Although their practical usage requires large-scale cell culture, scaling up of conventional adherent cultures is extremely challenging, as uniform high quality, reproducibility, and low running and labor costs must all be achieved. Recently, hPSC suspension cultures (Amit et al., 2010; Chen et al., 2012; Olmer et al., 2010; Singh et al., 2010; Steiner et al., 2010) have attracted considerable attention. They can potentially be scaled up because attachment surfaces and adhesion molecules are unnecessary, resulting in reduced good-manufacturing-practice-grade components and production costs. However, the limitations of current suspension culture methods include suboptimal passaging procedures that require dissociation and reaggregation and uncontrollable spontaneous fusion between cell aggregates (Amit et al., 2010; Olmer et al., 2010; Singh et al., 2010; Steiner et al., 2010). Enzyme treatments that dissociate hPSC colonies into single cells or small aggregates for subculturing induce considerable hPSC loss due to the sensitivity of these cells to physical stresses and single-cell dissociation (Singh et al., 2010; Steiner et al., 2010). Thus, enzymatic treatment may be the major reason for relatively low cell expansion ratios in suspension culture (Amit et al., 2010, 2011; Chen et al., 2012; O'Brien and Laslett, 2012; Olmer et al., 2010; Serra et al., 2012; Singh et al., 2010; Steiner et al., 2010; Zweigerdt et al., 2011). Another problem with suspension cultures is fusion between cell aggregates (Serra et al., 2012; Zweigerdt et al., 2011). Uncontrollable spontaneous fusion causes variation in sphere sizes; the formation of very large spheres may cause unwanted cell death and/or spontaneous differentiation (Bauwens et al., 2008).

For the practical application of hPSCs in cell therapy or drug discovery, further refinements toward large-scale, 3D culturing systems are desired. Current versions of 3D culture systems for large-scale hPSC production include dynamic stirring of carrier beads or cell aggregates in spinner flasks or their equivalents (Abbasalizadeh et al., 2012; Amit et al., 2010, 2011; Chen et al., 2012; Krawetz et al., 2010; Olmer et al., 2010, 2012; Singh et al., 2010; Zweigerdt et al., 2011). Such stirring, however, needs to be fine-tuned to minimize detrimental shearing forces that cause significant physical damage to hPSCs (Abbasalizadeh et al., 2012; Amit et al., 2011; O'Brien and Laslett, 2012; Singh et al., 2010).

We report here a novel 3D sphere culture system using mechanical passaging and functional polymers that

resolves major problems associated with suspension culture methods and dynamic stirring systems. This system may be optimized toward translation into a large-scale hPSC production format.

RESULTS

Subculture Method Using Mesh Filters

We developed a subculture method for hPSC suspension culture based on the mechanical disruption of cell aggregates into smaller aggregates. Larger cell spheres can be fragmented into smaller ones by simply passing them through a mesh filter of the appropriate pore size. This is a much simpler and easier procedure than enzymatic dissociation (Figures 1A and 1B). However, immediately after the passaging, the smaller spheres exhibited significant cell loss, which may be due to physical injury. To decrease the cell loss, we added a ROCK inhibitor (Ri), which increases survival of hPSCs after dissociation into single cells (Watanabe et al., 2007), for around 24 hr after subculturing (Figure S1A available online).

We tested several mesh sizes for optimal subculturing. The fold increase in cell number from day 0 to day 5 was dependent on the mesh size, as larger mesh sizes produced larger spheres with minimal cell loss (Figure S1B). However, using 70 μm meshes resulted in spheres diameter over 300 μm within 5 days, with dark spots appearing within these spheres (Figure S1C). Because the rate of apoptosis has been reported to increase with larger sphere diameter (Amit et al., 2010), this may indicate spontaneous necrosis or differentiation due to increased sphere size. Thus, when meshes over 70 μm are used, subculture is required every 3 days, causing frequent cell loss. On the other hand, smaller mesh sizes could produce smaller spheres, which might allow for greater expansion of cell numbers between subcultures. However, during our testing, the smaller spheres showed a decreased fold increase in cell numbers compared to the larger mesh sizes, presumably due to the inability of Ri to completely block cell death in these smaller sphere. Ultimately, we chose 50 μm as the optimal mesh size for subculture. After passaging, these meshes produced spheres with a diameter of around 80 μm that expanded into larger spheres of 220–250 μm in 4 or 5 days, depending on the cell line. When such spheres were allowed to grow further, many reached diameters of >300 μm (Figures S1D and S1E). Thus, we determined an optimal subculturing cycle of 4 or 5 days to avoid the production of oversized spheres (Figures 1B and S1D).

Fusion Suppression with Methylcellulose Polymer

Another significant problem with suspension cultures is spontaneous fusion between cell aggregates (Serra et al., 2012; Zweigerdt et al., 2011). To reduce aggregate fusion, we tested the addition of various nontoxic polymers to the culture medium and found that methylcellulose (MC) yielded encouraging results (Figure 1C). MC is widely used for cell culture, including for hematopoietic cells, and is known to be nontoxic to many cell types (Miyamoto et al., 1989; Ogawa et al., 1976).

We then optimized the concentration of MC. Whereas higher concentrations reduced fusion more strongly, collecting the spheres via centrifugation for culture media exchange or subculturing was hampered by the resulting increase in viscosity. We found that a concentration of 0.3%–0.6% (w/v) MC is adequate as the best compromise between the fusion repression and viscosity increase. These concentrations of MC are lower than the typical working concentration (1%) frequently used in the hematopoietic cell culture (Jin et al., 2013; Lu et al., 2007), and thus, the lower viscosity results in easy handling during medium changing, etc. Use of this concentration range decreased the average fusion rate from 14.9% (SD: ±5.5%) to 9.2% (SD: ±2.4%) in the case of the hiPSC line 253G1 ($n = 5$; $p < 0.1$; Figure 1C) and from 13.7% (SD: ±4.5%) to 2.4% (SD: ±1.4%) for the hESC line H9 ($n = 6$; $p < 0.001$) from independent experiments. Flow cytometry analysis revealed that over 90% of the cell population expressed pluripotency surface markers in H9 spheres cultured in the medium supplemented with 0.6% MC that reduced spontaneous sphere fusion. On the other hand, these ratios decreased below 90% in the spheres cultured without MC (Figure S1F). Thus, addition of MC was beneficial for suppression of spontaneous fusion and maintenance of the pluripotency.

Sphere Culture Protocol and Expansion Rate

With these improvements in sphere culture, the hPSCs grew as spherical aggregates of uniform size that could be subcultured every 4 or 5 days. The initial seeding density was adjusted to $0.7–1.0 \times 10^5$ cells/ml. First, we used the hESC line KhES-1 and mTeSR culture media. Although the small aggregates appeared elliptical immediately after passaging, they became spherical after 4 hr (Figure 1B). The distribution of sphere size was relatively homogeneous and constituted a near-normal distribution and with an average diameter between 90 μm and 270 μm within 7 days (Figures 1B, S1D, and S1E). The cell number increased exponentially until d6 (Figure S2A). Therefore, we chose the subculture cycle of 4 or 5 days before reaching plateau. During the 4- or 5-day intervals of sphere growth, the cell number increased 10- to 20-fold, depending on the cell line (Figure S2B). Our method is broadly applicable, as it was successful for all other tested hPSC lines, including the hESC lines KhES-3, H9, and HES3 and the hiPSC lines IMR90-1 and 253G1 (Figures S2B and S2C).

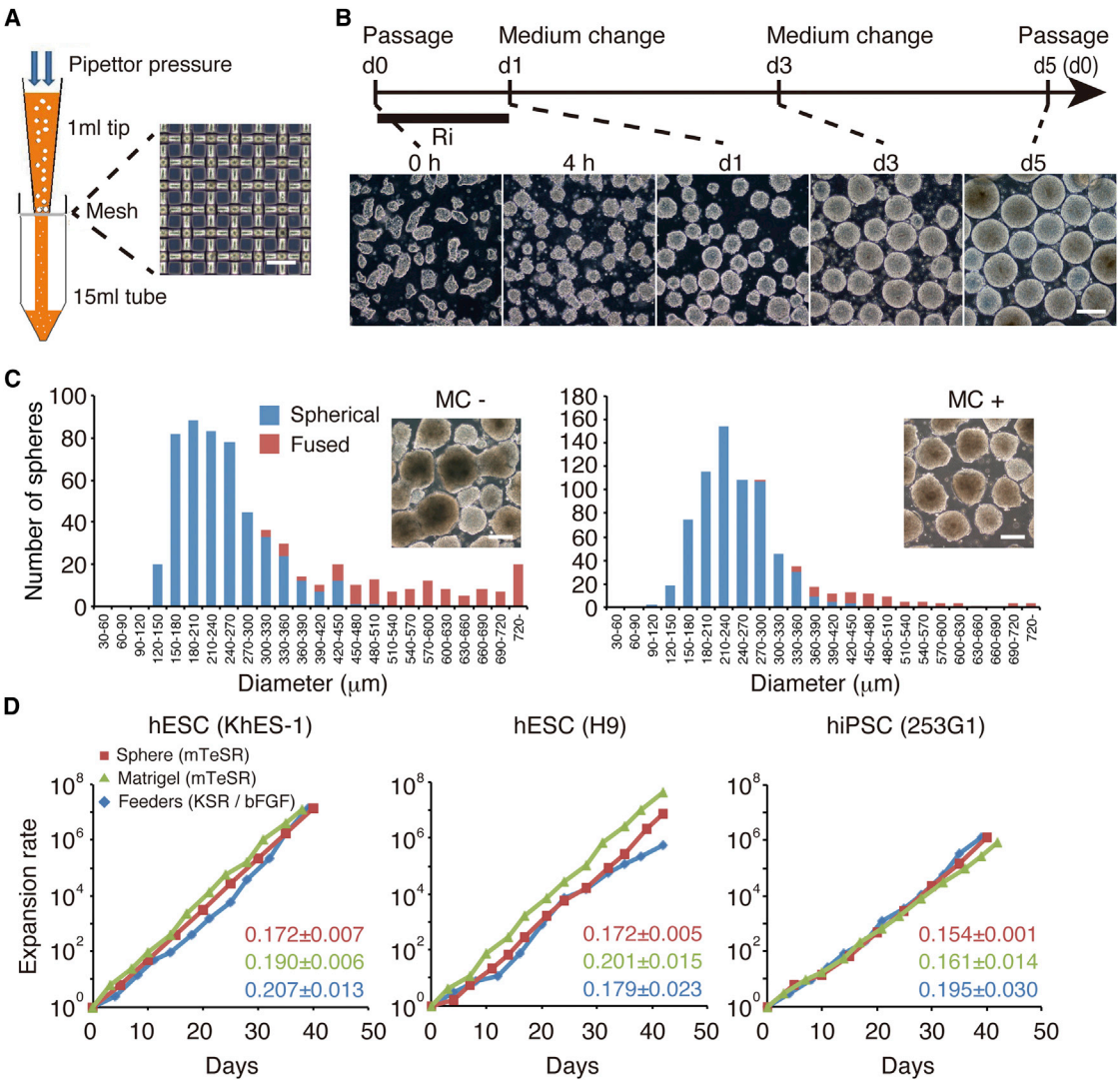

Figure 1. Sphere Culture of Human Pluripotent Stem Cells

(A) Mechanical subculture by passaging the cells through mesh filters. Spheres are pushed through a mesh filter with an opening size of 50 μm using a 1 ml micropipette tip. The scale bar represents 100 μm.

(B) Subculture cycle and shapes of spheres of the KhES-1 cell line during the 5-day interval. The scale bar represents 200 μm.

(C) Size distribution and morphology of cells from the 253G1 cell line in culture media with or without 0.3% methylcellulose on day 5. The blue and red bars represent the number of spherical and fused spheres in each size range, respectively. The graphs show exemplary one of the five independent experiments. The scale bars represent 200 μm.

(D) Comparison of expansion rates of the KhES-1, H9, and 253G1 cell lines in the sphere culture or in the conventional adherent culture on feeder layers or on Matrigel. The graph shows exemplary expansion rate plotting. Average slopes and SD in the semilogarithmical plotting were obtained by calculating exponential trend lines from three independent experiments and indicated in each graph.

See also Figures S1, S2, and S4.

We compared the expansion rate of the cells in the sphere culture and conventional adherent culture over 1 month. The expansion rate was calculated by multiplying the split ratios at each passage, and it was similar to the conventional adherent culture on feeder cells with knockout serum replacement (KSR)/basic fibroblast growth factor (bFGF) medium or on Matrigel with mTeSR medium (Figure 1D). In fact, slopes in the semilogarithmical plotting of the expansion rate were similar between the sphere and adherent cultures. Thus, our sphere culture system can expand all of the tested hPSC lines, with their expansion rates of 8.1×10^6 (SD: $\pm 4.3 \times 10^6$; KhES-1), 1.4×10^6 (SD: $\pm 0.2 \times 10^6$; 253G1), and 16.5×10^6 (SD: $\pm 6.6 \times 10^6$; H9) during

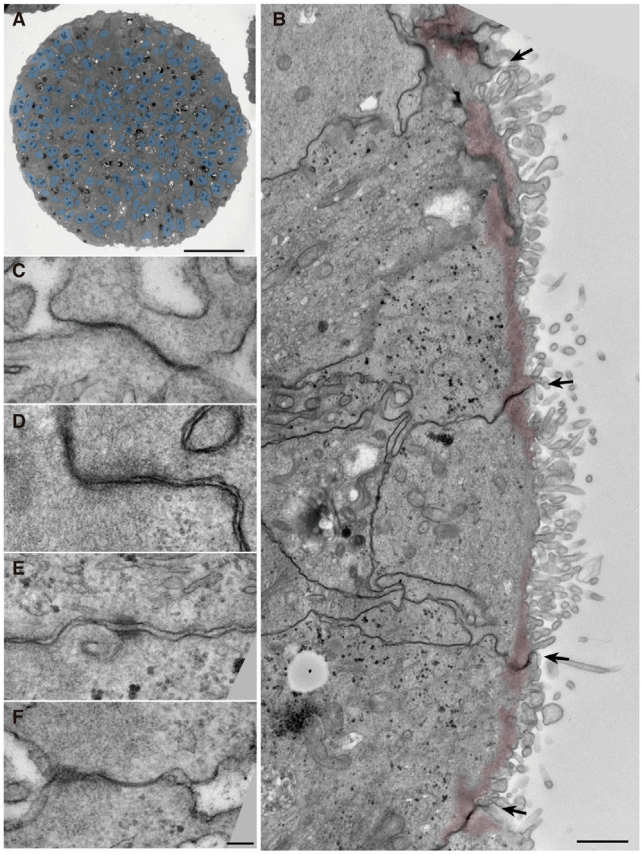

Figure 2. Transmission Electron Microscopy of Human Pluripotent Stem Cell Spheres

(A) A low-magnification (light microscopy) image of a KhES-1 sphere at four passages. The blue signal indicates nuclei. The scale bar represents 50 μm.

(B) A high-magnification image of the peripheral region of a KhES-1 sphere. The black arrows indicate adherens junctions, and the red signal indicates actin bundles. The black dots indicate glycogen granules. The scale bar represents 1 μm.

(C–F) Higher magnification images of a (C) tight junction, (D) adherens junction, (E) desmosome, and (F) gap junction found in the periphery of a KhES-1 sphere. The scale bar represents 100 nm.

40 days (42 days for the H9 line) from three independent experiments (n = 3).

Sphere Morphology and Expression of Pluripotency Markers

When we examined the spheres using electron microscopy, we found that they were composed of uniform cells with no significant differentiation characteristics (Figures 2A and 2B). The sphere surface was covered with numerous microvilli (Figure 2B). We noticed the presence of junction complexes on the sphere surfaces that were reminiscent of the apical side of an epithelium (Figures 2B–2F). These complexes included tight junctions, adherens junctions, desmosomes, and gap junctions. Immunostaining of frozen sections showed that all of the cells in a sphere expressed pluripotency marker molecules, including OCT3/4, NANOG, SSEA-4, and TRA-1-60 (Figures 3A and S3A). Flow cytometric analysis revealed that over 95% of the cell population expressed pluripotency surface markers. The fluorescent staining intensities and distribution of the pluripotency markers in populations were identical to those observed in conventional adherent cultures (Figures 3B and S3B).

StemPro Medium Compared with mTeSR Medium

We also examined whether our sphere culture method was compatible with other established media. We confirmed that StemPro medium (Life Technologies), could be used, although the growth rate of the spheres was reduced when this medium was used. Because the standard concentration of bFGF in the StemPro medium (8 ng/ml) is much lower than that of mTeSR (100 ng/ml), we tested higher concentrations and obtained better growth rates (Figures S4A and S4B). Although the spheres that formed in StemPro exhibited slightly different morphology, the addition of 50 ng/ml bFGF resulted in a growth rate that was similar to that observed in mTeSR (Figure S4B). We also confirmed that almost all of the cells in the spheres grown under these conditions expressed pluripotency surface markers (Figure S4C). Although we obtained similar results using either mTeSR or StemPro, we decided to use mTeSR for further investigation, as the latter medium yielded a slightly larger cell population.

Characterization of hPSC Spheres

Upon examination after middle- to long-term subculturing (around 20 or 50 passages) for the sphere culture, the karyotypes of the hPSCs were found to be normal (Figures 3C and S5A). These spheres could be transferred to the conventional adherent culture either on feeder cells or Matrigel. We also confirmed that the spheres could be cryopreserved and thawed through the standard vitrification method to restart either the sphere or adherent culture. The viability of the frozen cells upon thawing was similar in both sphere and adherent cultures, at 88.4% (SD: ±1.8%) and 90.3% (SD: ±2.2%) from three independent experiments, respectively.

We examined the differentiation potential of hPSCs in our sphere culture through an in vitro differentiation assay and an in vivo teratoma formation assay. The induction of early lineage marker expression for the three germ layers was confirmed by embryoid body (EB) formation (Figures S5B and S5C). The cells differentiated in culture into cardiomyocytes that expressed the cardiac markers cardiac troponin T, α-actinin, and NKX2.5 and also into neurons that expressed the neural marker βIII tubulin (Figures S5D

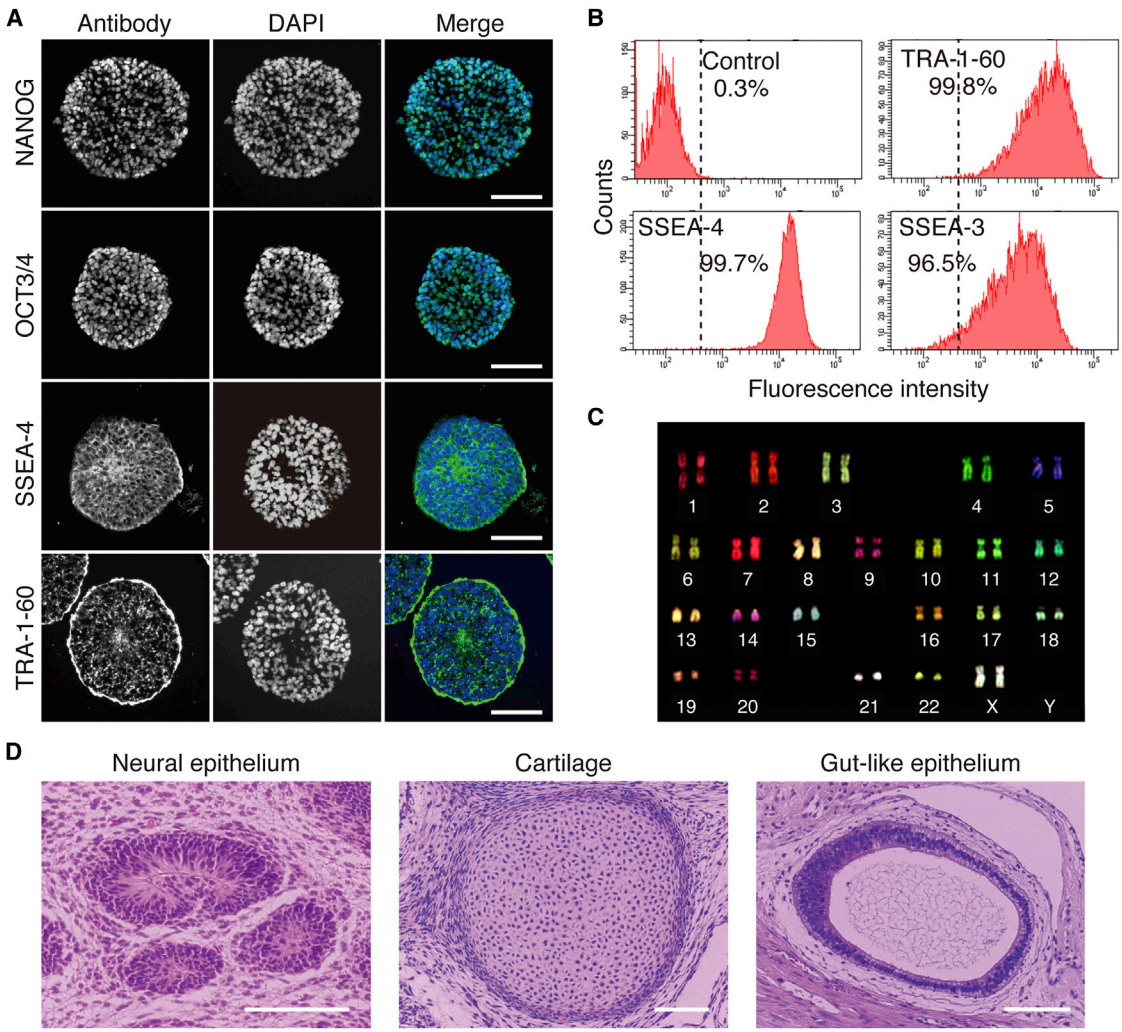

Figure 3. Pluripotency Marker Expression and Karyotype of Human Pluripotent Stem Cells in Sphere Culture

(A) Immunofluorescent staining of pluripotency marker proteins NANOG, OCT3/4, SSEA-4, and TRA-1-60 in frozen sections of KhES-1 spheres after 55 passages. In the merged panels, the green signals indicate the markers and the blue signals indicate DAPI nuclear staining. The scale bar represents 100 μm.

(B) Flow cytometry analysis of the pluripotency surface markers SSEA-4, TRA-1-60, and SSEA-3 on KhES-1 cells in the sphere culture after 72 passages. The control panel indicates analysis without the primary antibody. The percentage of the marker-positive population is indicated in each panel.

(C) Multicolor FISH karyotype analysis of sphere-cultured KhES-1 cells at passage 51.

(D) Histology of teratomas derived from KhES-1 cells at passage 21 in the sphere culture. The teratomas contained various tissues from the three germ layers, including the neural epithelium (ectoderm), cartilage (mesoderm), and gut-like epithelium with mucosa (endoderm). The scale bars represent 50 μm.

See also Figures S3–S5.

and S5E). When transplanted into immune-deficient mice, hPSCs in sphere cultures formed typical teratomas that contained tissues of all three germ layers, including the neural epithelium, cartilage, and gut-like epithelium (Figure 3D). Taken together, these data indicate that our sphere culture system supports robust growth and the pluripotency of all tested hPSC lines.

Gellan Gum Polymer Inhibits Sedimentation

For the practical application of hPSCs, further progress toward large-scale, 3D culture system is required. Therefore, we searched for additional chemical compounds that could maintain the hPSC spheres in suspension without the need for stirring, which causes significant cell damage (Abbasalizadeh et al., 2012; Amit et al.,

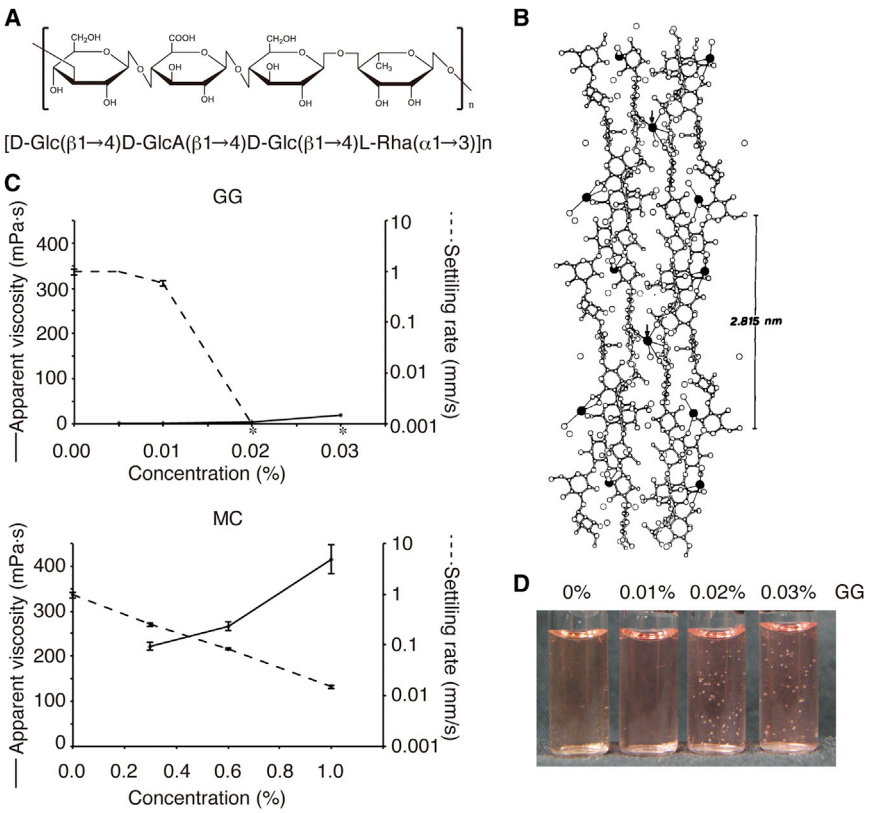

Figure 4. Characterizations of Low-Acyl Gellan Gum Polymer

(A) The chemical structure of the repeat unit of low-acyl gellan gum (GG).

(B) Stereo view of GG (reproduced from Figure 2 in Chandrasekaran and Thailambal, 1990). Two adjacent up- and down-pointing gellan double-helices are crosslinked at the arrows by calcium ions (filled circles).

(C) Apparent viscosities and settling rates of GG and methylcellulose (MC). The average and SD are shown from three experiments (n = 3). The asterisks indicate no settling.

(D) Settled or suspended polystyrene beads in the culture medium under various concentrations of GG.

2011; O'Brien and Laslett, 2012; Singh et al., 2010). We tested several large-molecule compounds for their ability to maintain polystyrene beads in suspension, because these beads have a diameter and specific gravity similar to those of hPSC spheres. We identified a polymer, low-acyl gellan gum (GG), which inhibits sedimentation and maintains the beads in suspension. GG was originally isolated as an extracellular polysaccharide secreted by *Sphingomonas paucimobilis* and is currently used widely as a natural food additive, owing to its unique physicochemical characteristics that add a distinct chewing texture (Bajaj et al., 2007). As shown in Figures 4A and 4B, GG consists of a linear anionic tetrasaccharide repeating unit, which forms double helical structures that assemble into firm and brittle aqueous gels in the presence of cationic ions (Chandrasekaran and Thailambal, 1990). Most of the polymers, such as MC, show elevated viscosity and handling difficulty with increasing concentration. Nevertheless, they cannot completely inhibit sedimentation (Figure 4C, lower panel). In contrast, addition of GG does not increase apparent viscosity but completely inhibits bead sedimentation at very low concentrations (i.e., approximately 0.02%; Figure 4C, upper panel). In such media, polystyrene beads remain in suspension without the need for dynamic agitation (Figure 4D).

3D Sphere Culture with GG Polymer

By utilizing the distinct properties of GG, we further improved our sphere culture system toward 3D culture without mechanical or dynamic stirring. As shown in Figure 5A, 3D sphere culture medium supplemented with 0.015%–0.02% GG can maintain sphere suspended for at least 2 days (48 hr). It shows no sign of gelation or significantly increased viscosity (Movie S1). Thus, for medium change or subculture, spheres can be collected quickly and simply by mild centrifugation after dilution with a double volume of Dulbecco's modified Eagle's medium (DMEM)/F12 basal medium. Then, we confirmed that hPSCs could proliferate at normal rates in the 3D sphere culture medium in culture plates (Figure 5B). We compared the mTeSR medium supplemented with MC and GG or GG only for the 3D culture medium. Growth rate in the MC+GG medium was slightly better than that in the GG-only medium (Figure S6A). Thus, we decided to use MC+GG medium for the 3D sphere culture medium. Also, we compared the passaging method either using mesh filters or single-cell dissociation and reaggregation in the 3D culture system. The single-cell dissociation method gave much lower growth rate than the filter mesh method (Figure S6B). It seems that the dissociated single cells cannot form adequate spheres in the 3D sphere culture medium. Thus, we confirmed that the passage

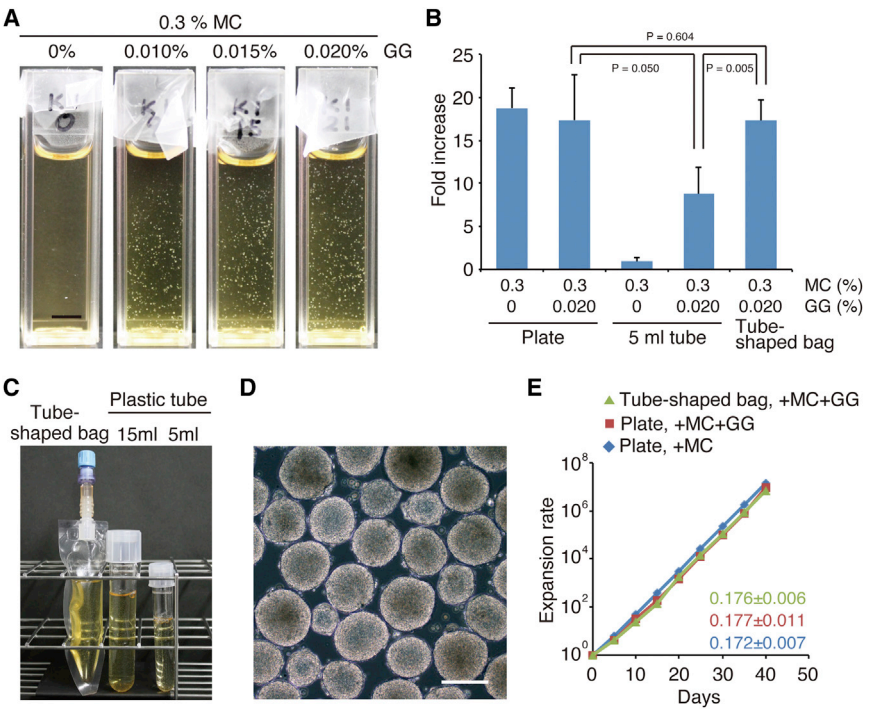

Figure 5. 3D Sphere Culture of Human Pluripotent Stem Cells

(A) Complete inhibition of hPSC sphere sedimentation by low-acyl GG at 0.015%. KhES-1 spheres on day 4 were suspended in the culture medium with various concentrations of GG and observed after 16 hr. The scale bar represents 5 mm.

(B) Fold increase in KhES-1 cell number in culture medium with or without GG in different culture vessels. The average fold increase from independent experiments indicates the cell number increase from days 0 to 5, and the error bars indicate the SD (n = 10 for tube-shaped bags and n = 4 for others). Significance calculations were performed using the Student's t test.

(C) A tube-shaped culturing bag made of a gas-permeable membrane (left) and polystyrene tubes (15 and 5 ml).

(D) Morphologies of KhES-1 spheres on day 5 in the 3D sphere culture medium with 0.020% GG. The scale bar represents 200 μm.

(E) Comparison of KhES-1 cell expansion rates in the 3D sphere culture using tube-shaped gas-permeable bags or culture plates. The graph shows exemplary expansion rate plotting. Average slopes and SD in the semilogarithmical plotting were obtained by calculating exponential trend lines from three independent experiments and indicated in each graph.

See also Figure S6 and Movie S1.

method using mesh filters is optimal for our 3D culture system.

To progress toward a practical larger-scale 3D culture system, we next examined hPSC culture in test tubes as a model of deep medium containers. Whereas the spheres that were cultured with 2D sphere culture medium settled to the bottoms of polystyrene tubes and underwent complete growth inhibition, spheres that were cultured in the 3D medium remained in suspension and grew at slower rates than cells in culture plates (Figure 5B). We speculated that the decreased cell growth may have been due to insufficient gas exchange and therefore used a tube-shaped bag that was made of a gas-permeable membrane (Nipro; Figure 5C). As expected, the spheres in the bag grew at growth rates similar to those of spheres in culture plates (Figure 5B). The morphologies and sizes of the spheres in 3D and 2D sphere culture medium were similar (Figure 5D), as was the expansion rate (Figure 5E). Cells also maintained a normal karyotype (Figures S6C).

The hPSCs from the 3D sphere culture expressed the pluripotency marker molecules OCT3/4, NANOG, SSEA-4, and TRA-1-60, as shown with immunostaining (Figures S6D and S6E). Over 95% of the cell population expressed pluripotency markers, as established by flow cytometry (Figure S6F). We also confirmed that the hPSCs could differentiate into cells that express lineage marker genes of the three germ layers in an EB formation assay (Figure S6G). These data thus indicate that our novel 3D culture system enables robust and stable hPSC growth and expansion while maintaining pluripotency.

Scaling Up of 3D Sphere Culture

To demonstrate the capability of scaling up our novel 3D sphere culture system, we tested 200 ml volume capacity culture bags that are made of a gas-permeable membrane. KhES-1 spheres were subcultured at 13.2×10^6 (SD: $\pm 5.0 \times 10^6$) cells/bag, and we changed the culture medium on days 1, 3, and 5. The growth rate in the bags was 12.5-fold (SD: ±4.9) on day 5, yielding 1.4×10^8 (SD: $\pm 0.1 \times 10^8$) cells per bag from three independent experiments (n = 3; Figure 6A).

Such cell number would be equivalent to the total number of cells harvested from 17 (SD: ±2) of the 100 mm culture dishes in conventional adherent culture system with daily medium change (Figure 6B). Thus, the cell number yield per volume of the consumed medium would be higher in the 3D culture system than that in conventional adherent culture. The morphologies and sizes of the

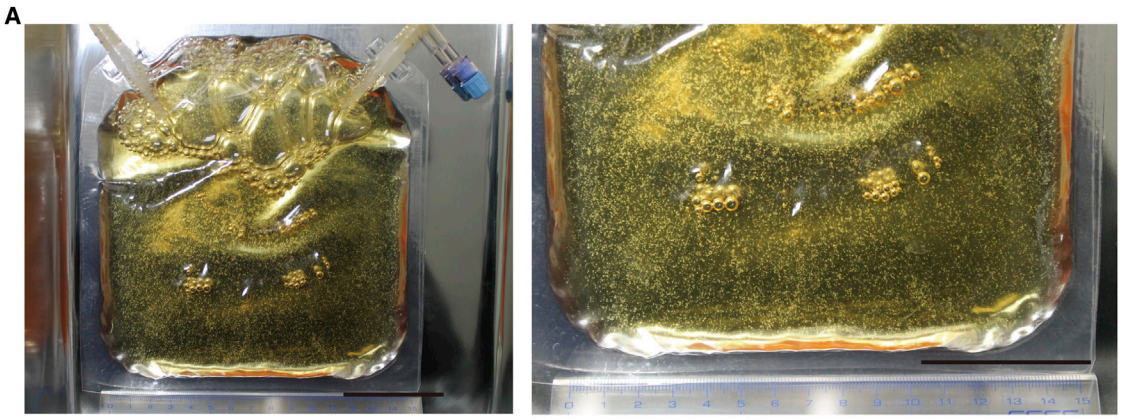

B

	200 ml culture bag	100 mm culture dish
Culture volume (ml)	200	10
Average cell number yield	1.4×10^8 / bag	8.3×10^6 / dish
Expected cell yield / 200 ml	1.4×10^8 / bag	1.7×10^8 / 20 dishes
Average cell number / ml	7.2×10^5 *	8.3×10^5 **

* Medium change : d1 and d3
** Medium change : daily

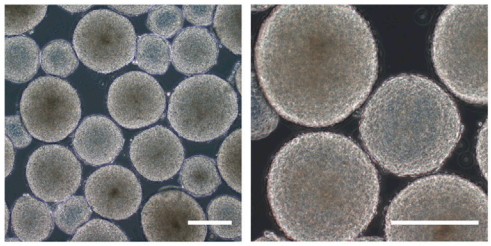

Figure 6. Proof of Principle 3D hPSC Sphere Culture
(A) A trial for larger-scale sphere culture by using 200 ml gas-permeable membrane bags. The scale bar represents 5 cm.
(B) Comparison of cell yield calculated from the average cell number obtained in the 3D sphere or adherent culture using KhES-1 cell line.
(C) Morphology of KhES-1 spheres cultured for 5 days in a 200 ml bag. The scale bar represents 200 μm.

spheres (Figure 6C) were similar to those of spheres in the small-scale culture. These results suggest that our 3D culture system may be used as a starting point for the large-scale culture aimed at practical applications in cell-based therapy or drug discovery.

DISCUSSION

In this study, we developed a simple, mechanical subculturing method that uses mesh filters and a polymer to suppress spontaneous cell aggregate fusion. In doing so, we believe we have resolved most of the major problems associated with current suspension culture system for hPSCs. The hPSCs form spheres of uniform size, expand robustly, and have stable growth rates that are similar to those of conventional adherent culture. Furthermore, by adding the GG polymer, which prevents sedimentation of the spheres without increase of the viscosity, we also succeeded in excluding the potentially damaging processes of dynamic agitation or stirring in 3D culture systems. The system thus provides a very simple and practical setup for large-scale hPSC expansion and production.

Depending on the disease target or therapy type, a large number of cells may be required for clinical applications involving hPSCs. For example, whereas relatively small numbers of cells (around 10^5 or 10^6) will be required for treating macular dystrophy (Serra et al., 2012) or Parkinson's disease (Lindvall et al., 2004; Serra et al., 2012), a much larger number of cells (between 10^9 and 10^{10}) will be necessary for treating myocardial infarction, hepatic failure, or diabetes (Jing et al., 2008; Lock and Tzanakakis, 2007; Serra et al., 2012). This creates a need for a robust and reliable large-scale cell culture and production system for realization of cell-based therapy using hPSCs.

Furthermore, this type of large-scale cell production system should have a high level of quality control for minimizing risks and quality variation in cell products. For example, a very large number of stem cells should be produced in a single culture vessel or bioreactor, rather than in multiple vessels, to assure that the whole product has the same characteristics as a single lot of stem cells or differentiated cells. Aliquots from this "master batch" can thus

be used for downstream safety characterization, such as tumor formation risk assessment. In order to apply such a large-scale culture system for hPSCs, this suspension culture system could be utilized for the optimal production system, as it avoids the need for costly extracellular matrix molecules for cell adhesion and for enzymatic cell dissociation that can compromise cell quality.

Here, we provide proof-of-principle that a gas permeable culture bag can be used in the 3D culture system, obviating the need for stirring during gas and nutrient exchange. We succeeded to use a 200 ml culture bag with a thickness of 15 mm for cell production. Thus, it would be possible to use a 1 l medium capacity culture bag of the same thickness, with increased scale of production of 1×10^9 cells per 1 l bag. Moreover, our novel 3D sphere culture system may be utilized for other mass-production systems such as bioreactors after additional research and development of the necessary adaptation technology. In such potential new types of bioreactors, our 3D culture medium using the GG polymer would enable to use minimum dynamic agitation only for keeping sufficient exchange of gases and nutrients in a bioreactor but no strong stirring necessary for keeping the spheres in suspension. In addition, the low viscosity of the 3D culture medium would not disturb the monitoring of culture parameters such as pH and pO2. Thus, these advantages can greatly reduce cell damages caused by shear stress of dynamic agitation in application to the bioreactor systems.

In summary, our novel 3D sphere culture system may be the optimal starting point for further development of large-scale hPSC production systems such as bioreactors and for practical large-scale applications in the cell therapy and drug discovery fields.

EXPERIMENTAL PROCEDURES

Human Pluripotent Stem Cell Lines

The hESC lines KhES-1, KhES-3, H9, and HES3 (Reubinoff et al., 2000; Suemori et al., 2006; Thomson et al., 1998) and the hiPSC lines 253G1 (Takahashi et al., 2007) and IMR90-1 (Yu et al., 2007) were used for this study. The hESC lines were used in accordance with the Guidelines for the Derivation and Utilization of Human Embryonic Stem Cells of the Ministry of Education, Culture, Sports, Science and Technology, Japan.

For the conventional adherent culture, hPSCs were grown on a mouse fibroblast feeder cell layer in DMEM/F12 with 20% KSR (Life Technologies) and 5 ng/ml recombinant bFGF (Wako Pure Chemical Industries) as reported previously (Suemori et al., 2006). For feeder-free adherent culture, hPSCs were grown on Matrigel (hESC-qualified Matrix, BD Biosciences) in mTeSR culture medium (STEMCELL Technologies).

Sphere Culture of Human Pluripotent Stem Cells

To initiate sphere cultures, hPSC colonies in conventional adherent cultures were partially dissociated into large clumps with CTK solution (Suemori et al., 2006) or dispase (BD Biosciences) and then rinsed with hPSC culture medium to remove the feeder cells. After collecting the clumps by centrifugation, they were suspended in the 2D sphere culture medium; mTeSR medium supplemented with 0.3%–0.6% MC (R&D Systems). Then, medium containing clumps of cells was supplemented with 10 μM Ri Y-27632 (Wako Pure Chemical Industries) in order to support cell survival in the subculture. Next, the clumps were passed through a nylon mesh filter with openings of 50 μm (CellTrics; PARTEC) and transferred to 6-well plates (Ultra Low Attachment Cluster Plate; Corning Life Sciences), with each well containing 3 ml of culture medium. The cell numbers were adjusted to 2 to 3×10^5 cells/well ($0.7–1.0 \times 10^5$ cells/ml). Under these culture conditions, the clumps became spherical after several hours. Culture medium was replaced on days 1 and 3 (day 0, subculturing day) by collecting the spheres through centrifugation and resuspending them in fresh, 2D sphere culture medium without Ri. The sphere diameters increased from around 80 μm on day 0 to over 200 μm on days 4 or 5. Spheres were subcultured every 4 (H9 cell line) or 5 (other hPSC lines) days; the spheres were collected by centrifugation and suspended in mTeSR with MC and Ri and were passed through a 50 μm mesh filter using a 1 ml Pipetman tip (Gilson). Alternatively, we also used 5 or 10 ml pipettes that were controlled by a motor-driven Pipettor (BD Falcon) for passaging through the mesh filters. The split ratios for each subculture were between 1:6 and 1:8, depending on the cell line. For cryopreservation, hPSC spheres on day 1 were frozen using a previously described vitrification cryopreservation method (Fujioka et al., 2004; Suemori et al., 2006).

3D Sphere Culture with Gellan Gum Polymer

The 3D sphere culture medium was prepared at Nissan Chemical Industries as follows. Kelcogel low-acyl GG CG-LA (Sansho) was suspended in pure water to 0.3% (w/v) and dissolved by stirring at 90°C. The aqueous solution was sterilized at 121°C for 20 min in an autoclave. Then, the solution was added to mTeSR basal medium at the given concentration with stirring at room temperature. The final 3D sphere culture medium consists of mTeSR medium with 0.3% MC and 0.01%–0.02% GG.

We also used low-attachment culture dishes (Corning Life Sciences; 641-05191), polypropylene test tubes (BD Biosciences; 352058 or 352057), and culturing bags that were made of a gas-permeable membrane (Nipro). The procedures for changing the culture medium and passaging with mesh filters were the same as for 2D sphere culturing, except for sphere collection. In brief, the culture medium was diluted with a double volume of DMEM-F12 basal medium, mixed by gently inverting the tube several times, and then centrifuged at 100–180 × *g* for 3 min. This allowed collection of 3D cultured spheres in three simple steps that took only 5–10 min. For larger volume culture using 200 ml bags, the culture medium was replaced on days 1 and 3 by collecting the spheres using cell strainer (BD Falcon).

Characterization of Human Pluripotent Stem Cells in Sphere Cultures

The diameters of the hESC and hiPSC spheres were measured and analyzed using photographs that were taken with a phase-contrast

inverted microscope (Olympus) and processed with ImageJ software (NIH; http://rsbweb.nih.gov/ij/). Cells were counted with NucleoCounter NC-200 (Chemometec) after dissociating the spheres into single cells with a 0.25% trypsin-EDTA solution. The fold increase in cell number was calculated by using the cell numbers on day 0 and day 5. The expansion rates were calculated by multiplying the split ratios at each passage. For the karyotype analysis, hPSC spheres on day 1 were transferred to an adherent culture on feeder layer for 48 hr and treated with colcemid (Nakalai Tesque) according to the manufacturer's instructions. Fifty randomly selected mitotic metaphase nuclei were analyzed by chromosome counting, after which ten nuclei were examined using multicolor fluorescence in situ hybridization (FISH) karyotype analysis. These analyses were carried out by Chromosome Science.

Electron Microscopy

hPSC spheres were chemically fixed with 2% glutaraldehyde in NaHCa buffer (100 mM NaCl, 30 mM HEPES, and 2 mM $CaCl_2$ at pH 7.4). The specimens were postfixed with 0.25% OsO4/0.25% $K_4Fe(CN)_6$, dehydrated with a graded ethanol series, and embedded in Araldite 502 resin (Polysciences). After polymerization at 65°C for a few days, ultrathin sections, obtained using a Ultramicrotome (Leica FC6), were mounted on EM grids, stained with lead citrate, and then observed with a conventional transmission electron microscope (JEOL JEM1400). Bright-field light microscopy images were obtained from thick sections (~1 μm) that had been stained with toluidine blue.

Marker Expression Analysis

For pluripotency marker immunostaining, hPSC spheres were fixed with 4% paraformaldehyde (PFA), rinsed in PBS, soaked in 15% sucrose, and embedded in optimum cutting temperature compound (Sakura Finetek) for frozen sectioning. Sphere samples were sectioned in 12-μm-thick slices, permeabilized and blocked with 1% BSA, and stained with primary antibodies as follows: rabbit anti-NANOG (Cell Signaling Technology), mouse anti-OCT3/4 (C-10; Santa Cruz Biotechnology), rat anti-SSEA3 (MC631; Millipore), mouse anti-SSEA4 (MC813; Millipore) or mouse anti-TRA-1-60 (Millipore). The samples were incubated with Alexa Fluor 488-conjugated secondary antibodies (Life Technologies), and signals were detected and photographed through fluorescence microscopy.

For flow cytometry analysis, hPSC spheres were dissociated into single cells with a 0.25% trypsin-EDTA solution for 2 min, rinsed with staining buffer (PBS with 2% fetal bovine serum [FBS]), and incubated for 30 min at 4°C with primary antibodies that had been diluted in the staining buffer. Then, the samples were rinsed with staining buffer, incubated for 30 min at 4°C with secondary antibodies that had been diluted in staining buffer, rinsed with staining buffer, and counterstained with 7-amino-actinomycin D (BD Biosciences) immediately before analysis. The stained cell samples were analyzed using a FACS Canto II Flow Cytometer and FACS Diva software (BD Biosciences).

For marker gene expression analysis, total RNA was purified with an RNeasy Mini Kit (QIAGEN). cDNA was then synthesized using the purified RNA and SuperScript III Reverse Transcriptase (Life Technologies). Quantitative RT-PCR (qRT-PCR) was performed with each gene-specific primer/probe mix (TaqMan Gene Expression Assays), TaqMan Universal PCR Master Mix, and a 7900HT Fast Real Time PCR System (Life Technologies) according to the manufacturer's instructions. The PCR data were analyzed using the comparative cycle threshold method (2 Δ/Δ CT), and all of the values were normalized with respect to *PP1A* expression.

Differentiation Assay

For the teratoma formation assay, hESC spheres were injected directly into the testes of severe combined immunodeficiency mice (NOD.CB17-*scid*; CLEA Japan). After 8 weeks, the resulting teratomas were surgically dissected out of the mice and fixed with 4% PFA. The samples were embedded in paraffin, sectioned into 5 μm slices, and stained with hematoxylin and eosin. All mouse works were approved by the Institutional Animal Ethics Committee of Kyoto University.

For embryoid body formation, hPSC spheres on day 0 were cultured for 2 weeks in DMEM/F12 medium that had been supplemented with 5% KSR or 20% FBS. The medium was changed three times a week. Total RNA was purified and gene expression was analyzed by performing qRT-PCR as described above.

Induction of differentiation into cardiomyocytes or neurons during culturing was carried out as described previously (Minami et al., 2012; Sakurai et al., 2010). Procedures for the immunostaining analysis of the differentiated cells were also described previously (Minami et al., 2012; Sakurai et al., 2010). The antibodies that were used for this analysis were anti-cardiac troponin T (Santa Cruz Biotechnology), anti-αactinin (Sigma-Aldrich), and anti-NKX2.5 (Abcam) for cardiomyocytes, and anti-βIII tubulin (Sigma-Aldrich) for neurons.

Physical Property Measurements of Gellan Gum Solution

Viscosity was measured by using an MCR 302 rheometer (Anton Paar), a 25 mm cone plate, and a gap of 0.107 mm. The apparent viscosities of the samples were assessed at 25°C with a shear rate of 10 s^{-1}.

For measuring settling rates, sample solutions were added to bottles that contained polystyrene beads (diameter of 0.2–0.3 mm; specific gravity of 1.04; Polysciences). After shaking the bottles, the settling velocity of the beads was measured at 25°C.

Statistical Analysis

Throughout this study, each experiment was independently performed at least three times. All of the results were expressed as the mean ± SD. The unpaired two-tailed Student's t test was used to compare the mean values of measurements. Differences were considered significant for $p < 0.05$.

SUPPLEMENTAL INFORMATION

Supplemental Information for this article includes six figures, one table, and one movie and can be found with this article online at http://dx.doi.org/10.1016/j.stemcr.2014.03.012.

AUTHOR CONTRIBUTIONS

N.N., T.G.O., and K.H. conceived and designed the experiments, and T.G.O., J.B., A.Y., and M.T. performed the experiments. T.G.O., K.H., and N.N. analyzed the data. D.T., M.T., I.M., Y.Y., K.A., J.E.H., and T.N. contributed reagents, materials, and analysis tools. T.G.O., K.H., and N.N. wrote the paper.

ACKNOWLEDGMENTS

We thank Rie Ayuzawa, Sumie Matusguchi, Ayako Mochizuki, Rie Tatsumi, Dongyi Yan, and Norie Tooi for their technical assistance and Kaori Yamauchi and Hideaki Kumagai for their help with the teratoma formation assay. This work was supported by a grant from the New Energy and Industrial Technology Development Organization (P10027 to N.N.). Findings in this paper have resulted in patent applications by Kyoto University and Nissan Chemical Industries. M.T. and T.N. are employees of Nissan Chemical Industries. D.T. and Y.Y. are employees of Nipro Corporation. N.N. is a founder and shareholder of a hESC/iPSC-related company, ReproCELL.

Received: November 13, 2013
Revised: March 27, 2014
Accepted: March 27, 2014
Published: April 24, 2014

REFERENCES

Abbasalizadeh, S., Larijani, M.R., Samadian, A., and Baharvand, H. (2012). Bioprocess development for mass production of size-controlled human pluripotent stem cell aggregates in stirred suspension bioreactor. Tissue Eng. Part C Methods *18*, 831–851.

Amit, M., Chebath, J., Margulets, V., Laevsky, I., Miropolsky, Y., Shariki, K., Peri, M., Blais, I., Slutsky, G., Revel, M., and Itskovitz-Eldor, J. (2010). Suspension culture of undifferentiated human embryonic and induced pluripotent stem cells. Stem Cell Rev. *6*, 248–259.

Amit, M., Laevsky, I., Miropolsky, Y., Shariki, K., Peri, M., and Itskovitz-Eldor, J. (2011). Dynamic suspension culture for scalable expansion of undifferentiated human pluripotent stem cells. Nat. Protoc. *6*, 572–579.

Bajaj, I.B., Survase, S.A., Saudagar, P.S., and Singhal, R.S. (2007). Gellan gum: fermentative production, downstream processing and applications. Food Technol. Biotechnol. *45*, 341.

Bauwens, C.L., Peerani, R., Niebruegge, S., Woodhouse, K.A., Kumacheva, E., Husain, M., and Zandstra, P.W. (2008). Control of human embryonic stem cell colony and aggregate size heterogeneity influences differentiation trajectories. Stem Cells *26*, 2300–2310.

Chandrasekaran, R., and Thailambal, V.G. (1990). The influence of calcium ions, acetate and L-glycerate groups on the gellan double-helix. Carbohydr. Polym. *12*, 431–442.

Chen, V.C., Couture, S.M., Ye, J., Lin, Z., Hua, G., Huang, H.-I.P., Wu, J., Hsu, D., Carpenter, M.K., and Couture, L.A. (2012). Scalable GMP compliant suspension culture system for human ES cells. Stem Cell Res. (Amst.) *8*, 388–402.

Fujioka, T., Yasuchika, K., Nakamura, Y., Nakatsuji, N., and Suemori, H. (2004). A simple and efficient cryopreservation method for primate embryonic stem cells. Int. J. Dev. Biol. *48*, 1149–1154.

Jin, L., Feng, T., Shih, H.P., Zerda, R., Luo, A., Hsu, J., Mahdavi, A., Sander, M., Tirrell, D.A., Riggs, A.D., and Ku, H.T. (2013). Colony-forming cells in the adult mouse pancreas are expandable in Matrigel and form endocrine/acinar colonies in laminin hydrogel. Proc. Natl. Acad. Sci. USA *110*, 3907–3912.

Jing, D., Parikh, A., Canty, J.M., Jr., and Tzanakakis, E.S. (2008). Stem cells for heart cell therapies. Tissue Eng. Part B Rev. *14*, 393–406.

Krawetz, R., Taiani, J.T., Liu, S., Meng, G., Li, X., Kallos, M.S., and Rancourt, D.E. (2010). Large-scale expansion of pluripotent human embryonic stem cells in stirred-suspension bioreactors. Tissue Eng. Part C Methods *16*, 573–582.

Lindvall, O., Kokaia, Z., and Martinez-Serrano, A. (2004). Stem cell therapy for human neurodegenerative disorders-how to make it work. Nat. Med. Suppl. *10*, S42–S50.

Lock, L.T., and Tzanakakis, E.S. (2007). Stem/Progenitor cell sources of insulin-producing cells for the treatment of diabetes. Tissue Eng. *13*, 1399–1412.

Lu, S.-J., Feng, Q., Caballero, S., Chen, Y., Moore, M.A.S., Grant, M.B., and Lanza, R. (2007). Generation of functional hemangioblasts from human embryonic stem cells. Nat. Methods *4*, 501–509.

Minami, I., Yamada, K., Otsuji, T.G., Yamamoto, T., Shen, Y., Otsuka, S., Kadota, S., Morone, N., Barve, M., Asai, Y., et al. (2012). A small molecule that promotes cardiac differentiation of human pluripotent stem cells under defined, cytokine- and xeno-free conditions. Cell Rep. *2*, 1448–1460.

Miyamoto, T., Takahashi, S., Ito, H., Inagaki, H., and Noishiki, Y. (1989). Tissue biocompatibility of cellulose and its derivatives. J. Biomed. Mater. Res. *23*, 125–133.

O'Brien, C., and Laslett, A.L. (2012). Suspended in culture—human pluripotent cells for scalable technologies. Stem Cell Res. (Amst.) *9*, 167–170.

Ogawa, M., Parmley, R.T., Bank, H.L., and Spicer, S.S. (1976). Human marrow erythropoiesis in culture. I. Characterization of methylcellulose colony assay. Blood *48*, 407–417.

Olmer, R., Haase, A., Merkert, S., Cui, W., Paleček, J., Ran, C., Kirschning, A., Scheper, T., Glage, S., Miller, K., et al. (2010). Long term expansion of undifferentiated human iPS and ES cells in suspension culture using a defined medium. Stem Cell Res. (Amst.) *5*, 51–64.

Olmer, R., Lange, A., Selzer, S., Kasper, C., Haverich, A., Martin, U., and Zweigerdt, R. (2012). Suspension culture of human pluripotent stem cells in controlled, stirred bioreactors. Tissue Eng. Part C Methods *18*, 772–784.

Reubinoff, B.E., Pera, M.F., Fong, C.Y., Trounson, A., and Bongso, A. (2000). Embryonic stem cell lines from human blastocysts: somatic differentiation in vitro. Nat. Biotechnol. *18*, 399–404.

Sakurai, K., Shimoji, M., Tahimic, C.G.T., Aiba, K., Kawase, E., Hasegawa, K., Amagai, Y., Suemori, H., and Nakatsuji, N. (2010). Efficient integration of transgenes into a defined locus in human embryonic stem cells. Nucleic Acids Res. *38*, e96.

Serra, M., Brito, C., Correia, C., and Alves, P.M. (2012). Process engineering of human pluripotent stem cells for clinical application. Trends Biotechnol. *30*, 350–359.

Singh, H., Mok, P., Balakrishnan, T., Rahmat, S.N.B., and Zweigerdt, R. (2010). Up-scaling single cell-inoculated suspension culture of human embryonic stem cells. Stem Cell Res. (Amst.) *4*, 165–179.

Steiner, D., Khaner, H., Cohen, M., Even-Ram, S., Gil, Y., Itsykson, P., Turetsky, T., Idelson, M., Aizenman, E., Ram, R., et al. (2010). Derivation, propagation and controlled differentiation of human embryonic stem cells in suspension. Nat. Biotechnol. *28*, 361–364.

Suemori, H., Yasuchika, K., Hasegawa, K., Fujioka, T., Tsuneyoshi, N., and Nakatsuji, N. (2006). Efficient establishment of human embryonic stem cell lines and long-term maintenance with stable karyotype by enzymatic bulk passage. Biochem. Biophys. Res. Commun. *345*, 926–932.

Takahashi, K., Tanabe, K., Ohnuki, M., Narita, M., Ichisaka, T., Tomoda, K., and Yamanaka, S. (2007). Induction of pluripotent stem cells from adult human fibroblasts by defined factors. Cell *131*, 861–872.

Thomson, J.A., Itskovitz-Eldor, J., Shapiro, S.S., Waknitz, M.A., Swiergiel, J.J., Marshall, V.S., and Jones, J.M. (1998). Embryonic stem cell lines derived from human blastocysts. Science *282*, 1145–1147.

Watanabe, K., Ueno, M., Kamiya, D., Nishiyama, A., Matsumura, M., Wataya, T., Takahashi, J.B., Nishikawa, S., Nishikawa, S.-i., Muguruma, K., and Sasai, Y. (2007). A ROCK inhibitor permits survival of dissociated human embryonic stem cells. Nat. Biotechnol. *25*, 681–686.

Yu, J., Vodyanik, M.A., Smuga-Otto, K., Antosiewicz-Bourget, J., Frane, J.L., Tian, S., Nie, J., Jonsdottir, G.A., Ruotti, V., Stewart, R., et al. (2007). Induced pluripotent stem cell lines derived from human somatic cells. Science *318*, 1917–1920.

Zweigerdt, R., Olmer, R., Singh, H., Haverich, A., and Martin, U. (2011). Scalable expansion of human pluripotent stem cells in suspension culture. Nat. Protoc. *6*, 689–700.